

# High-voltage quasi-vertical GaN-on-Si Schottky barrier diode with edge termination structure of optimized multi-level N ion implantation

Qingyuan CHANG<sup>1</sup>, Bin HOU<sup>1\*</sup>, Ling YANG<sup>1</sup>, Mei WU<sup>1</sup>, Meng ZHANG<sup>1</sup>, Hao LU<sup>1</sup>,  
Fuchun JIA<sup>2</sup>, Xuerui NIU<sup>1</sup>, Chunzhou SHI<sup>3</sup>, Jiale DU<sup>1</sup>, Mao JIA<sup>1</sup>, Qian YU<sup>1</sup>,  
Shiming LI<sup>1</sup>, Youjun ZHU<sup>1</sup>, Xiaohua Ma<sup>1</sup> & Yue HAO<sup>1</sup>

<sup>1</sup>School of Microelectronics, Xidian University, Xi'an 710071, China;

<sup>2</sup>The 29th Research Institute of China Electronics Technology Group Corporation, Chengdu 610036, China;

<sup>3</sup>School of Advanced Materials and Nanotechnology, Xidian University, Xi'an 710071, China

Received 25 April 2024/Revised 6 July 2024/Accepted 20 September 2024/Published online 15 November 2024

GaN has several advantages, such as a large bandgap (3.44 eV), high critical electric field (3.3 MV/cm), and high carrier mobility (900 cm<sup>2</sup>/Vs), making it a strong candidate for next-generation high-power applications. In recent years, vertical Schottky barrier diodes (SBDs) have garnered significant attention due to their ability to achieve high breakdown voltage in small device sizes, insensitivity to surface states, improved heat dissipation, and enhanced reliability, distinguishing them from lateral diodes. However, the small size and high cost of GaN substrates limit large-scale production, leading to the preference for silicon (Si) substrates, which offer larger sizes, lower costs, and better compatibility [1]. Nevertheless, the presence of a peak electric field at the Schottky contact edge of SBDs leads to premature breakdown of the device and hampers the full utilization of the inherent advantages of GaN materials [2]. Numerous international publications have addressed the suppression of the electric field crowding effect in SBDs, employing techniques such as field plates, ion implantation, plasma treatment, and PN junction terminal [3]. Moreover, the impact of the NET terminal and the depth of NET (i.e. depth of high-resistance region) on the peak electric field at the Schottky contact edge of quasi-vertical GaN-on-Si SBD has not been thoroughly investigated, making it of significant importance.

In this work, a high-performance quasi-vertical GaN-on-Si SBD with NET was successfully fabricated. The thickness of the high-resistance region prepared in the final experiment is about 330 nm. The final prepared quasi-vertical GaN-on-Si SBD with NET exhibited exceptional characteristics, including a low turn-on voltage ( $V_{on}$ ) of 0.62 V, a specific on-resistance ( $R_{on,sp}$ ) of 1.06 m $\Omega$ ·cm<sup>2</sup>, a high breakdown voltage (BV) of 590 V, and a BFOM of 0.33 GW/cm<sup>2</sup>.

**Experiment.** Details of the device fabrication process and the optimization of the high-resistance region depth can be found in Appendixes A and B of the supplementary materials.

**Results and discussion.** The structural diagrams of quasi-

vertical GaN-on-Si SBD without and with NET are shown in Figures 1 (a) and (b), respectively. When high-energy N ions are injected into GaN, they disrupt the Ga-N bonds within the GaN lattice, leading to the formation of defects and impurities, as depicted in Figure 1 (c). These defects and impurities give rise to deep-level traps and contribute to the generation of high resistance region [4]. Figure 1 (d) clearly reveals the lattice disorder region resulting from N ion implantation (NII), giving rise to the formation of a uniform high-resistance region with an approximate thickness of 330 nm.

The surface roughness before and after NII was characterized using AFM, as shown in Figures 1 (e) and (f). It was found that the average roughness ( $R_a$ ) of GaN without NII is 0.172 nm, and the root mean square roughness ( $R_q$ ) is 0.216 nm. For GaN with NII,  $R_a$  is 0.198 nm, and  $R_q$  is 0.246 nm. The roughness increased slightly. This proves that NII has some weak effects on GaN surface. XRD analysis was conducted on GaN before and after NII, as shown in Figures 1 (g) and (h). The FWHM of the rocking curves for the (002) and (102) planes of GaN without NII are 223 and 256 arcsec, respectively, while for GaN with NII, the FWHM of the rocking curves for the (002) and (102) planes are 274 and 418 arcsec, respectively. Since the FWHM of the (002) rocking curve is only related to the screw dislocation density in the GaN film, while the FWHM of the (102) rocking curve is related not only to the screw dislocation density but also to the edge dislocation density in the GaN film [5]. After calculation, the screw dislocation density of GaN without NII is  $9.927 \times 10^7$  cm<sup>-2</sup>, and the edge dislocation density is  $4.426 \times 10^8$  cm<sup>-2</sup>. For GaN with NII, the screw dislocation density is  $1.499 \times 10^8$  cm<sup>-2</sup>, and the edge dislocation density is  $1.526 \times 10^9$  cm<sup>-2</sup>, indicating a 50% increase in screw dislocation density and a 240% increase in edge dislocation density. The TEM sample with NII was further observed and analyzed. After the TEM sample was prepared in the black box area of Figure 1(i), TEM observations were performed at 36000 $\times$ , revealing a clear lattice

\* Corresponding author (email: houbinme@163.com)

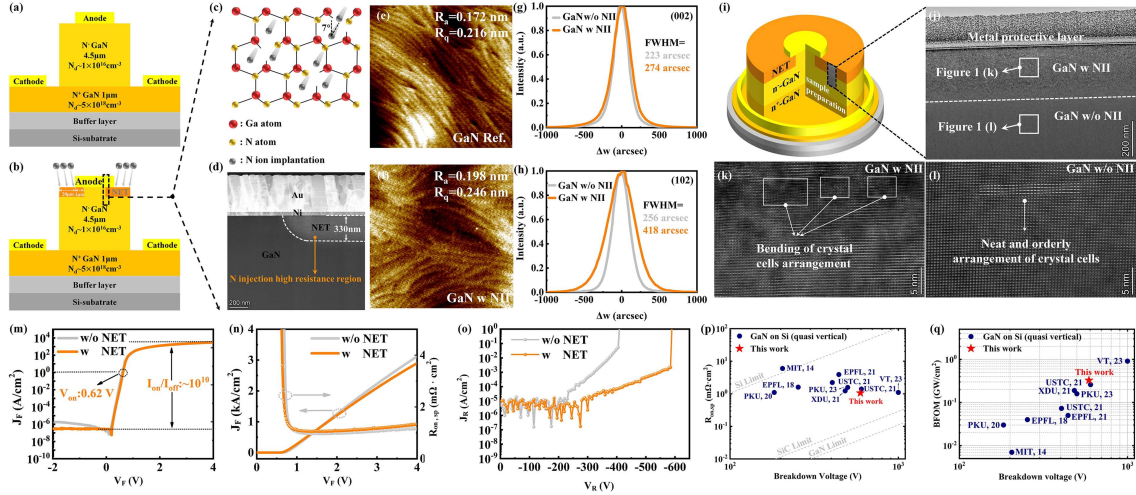


**Figure 1** (Color online) Schematic diagram of GaN SBD (a) without and (b) with NET. (c) Concept diagram of the mechanism of NII interrupting Ga-N bonding to form a high resistance region. (d) TEM schematic diagram of effective NII region at  $68000 \times$  and  $9400 \times$  in high-angle annular dark field (HAADF) mode. AFM characterizations of GaN (e) without and (f) with NII. Rocking curves for (g) the (002) plane and (h) the (102) plane of GaN without and with NII, respectively. (i) Three-dimensional cross-sectional structure diagram for GaN SBD with NET and TEM sample preparation area of GaN SBD with NET. (j) TEM image of the sample at  $36000 \times$ . TEM images of the sample (k) with and (l) without NII at  $1.05 \text{ M} \times$  magnification, respectively. Comparison of forward I-V characteristics of GaN SBD with and without NET in (m) semi logarithmic and (n) linear coordinates. (o) Comparison of reverse I-V characteristics of GaN SBD with and without NET in logarithmic coordinates. Comparison of SBD using NET structure with quasi vertical and fully vertical SBDs reported domestically and internationally under (p)  $R_{\text{on,sp}}$  versus breakdown voltage and (q) BFOM versus breakdown voltage coordinates.

disorder region, as shown in Figure 1 (j). Figure 1 (k) and Figure 1 (l) display TEM images of regions with and without NII at  $1.05 \text{ M} \times$ , respectively. The results indicate that the GaN material exhibits a more orderly cell arrangement in the region without NII. In the region with NII, obvious lattice defects are observed, and the arrangement of crystal cells is distorted to a certain extent.

Figures 1 (m) and (n) show a comparison of the forward I-V characteristics of GaN SBD with and without NET. The  $V_{\text{on}}$  of both devices are  $0.62 \text{ V}$ . In addition, the device with NET achieves lower off-state leakage current and higher  $I_{\text{on}}/I_{\text{off}}$ , which is about  $10^{10}$ . When the forward voltage of SBD with NET increases to  $4 \text{ V}$ , the current density can reach  $2.9 \text{ kA/cm}^2$ , which is  $0.2 \text{ kA/cm}^2$  less than the SBD without NET. This is because NII can disrupt the GaN lattice structure, thereby reducing carrier mobility, and the deep level traps introduced by NII can also have a certain impact on carrier concentration, increasing  $R_{\text{on,sp}}$  from  $0.97 \text{ m}\Omega\text{-cm}^2$  to  $1.06 \text{ m}\Omega\text{-cm}^2$ . Figure 1 (o) is a schematic diagram of the reverse I-V characteristics of the device. The BV of GaN SBD with NET can reach up to  $590 \text{ V}$  ( $1 \text{ A/cm}^2$ ), while GaN SBD without NET has a BV of  $410 \text{ V}$ . The NET can effectively increase the BV of the device and reduce the reverse leakage current. Figures 1 (p) and (q) benchmark  $R_{\text{on,sp}}$  versus BV and BFOM versus BV for the quasi-vertical GaN-on-Si SBD, respectively. Compared with other quasi-vertical GaN-on-Si SBDs, the GaN SBD with NET in this study has an international first-class BV of  $590 \text{ V}$ . At the same time, the  $R_{\text{on,sp}}$  of the device is  $1.06 \text{ m}\Omega\text{-cm}^2$ , and the final BFOM of the device reaches  $0.33 \text{ GW/cm}^2$ .

**Conclusion.** In summary, we optimized the depth of the high-resistance region using Silvaco software and achieved the corresponding depth of the high-resistance region by optimizing multi-level NII using SRIM software. We suc-

cessfully prepared quasi-vertical GaN-on-Si SBD with NET using quadruple NII. The GaN SBD with NET achieved excellent performance with  $R_{\text{on,sp}}$  of  $1.06 \text{ m}\Omega\text{-cm}^2$ ,  $V_{\text{on}}$  of  $0.62 \text{ V}$  and BFOM of  $0.33 \text{ GW/cm}^2$ . This proves the enormous potential of NET terminals in the field of quasi-vertical GaN-on-Si power devices.

**Acknowledgements** This work was supported by the National Natural Science Foundation of China (Grant Nos. 62474135, 62104184, 62234009, 62090014, 62188102, 62104178, 62104179) and the Fundamental Research Funds for the Central Universities of China (Grant Nos. YJSJ23019, XJSJ23047).

**Supporting information** Appendixes A and B. The supporting information is available online at [info.scichina.com](http://info.scichina.com) and [link.springer.com](http://link.springer.com). The supporting materials are published as submitted, without typesetting or editing. The responsibility for scientific accuracy and content remains entirely with the authors.

## References

- Zhang Y, Dadgar A, Palacios T. Gallium nitride vertical power devices on foreign substrates: a review and outlook. *Journal of Physics D: Applied Physics*, 2018, 51: 273001
- Chen J, Song X, Liu Z, et al. A GaN-on-Si quasi-vertical Schottky barrier diode with enhanced performance using fluorine ion-implanted field rings. *Applied Physics Express*, 2021, 14: 116504
- Fu H, Fu K, Chowdhury S, et al. Vertical GaN power devices: device principles and fabrication technologies art I. *IEEE Transactions on Electron Devices*, 2021, 68: 3200–3211
- Guo X, Zhong Y, Zhou Y, et al. Nitrogen-implanted guard rings for 600-V quasi-vertical GaN-on-Si Schottky barrier diodes with a BFOM of  $0.26 \text{ GW/cm}^2$ . *IEEE Transactions on Electron Devices*, 2021, 68: 5682–5686
- Heying B, Wu X H, Keller S, et al. Role of threading dislocation structure on the x-ray diffraction peak widths in epitaxial GaN films. *Applied Physics Letters*, 1996, 68: 643–645